



PO Box 1127
Rotorua 3040
Ph: + 64 7 921 1883
Fax: + 64 7 921 1020
Email: info@ffr.co.nz
Web: www.ffr.co.nz

Theme: Radiata Management

Task No: F10203
Milestone Number: 2

Report No. FFR- R006

Mechanics of the Stem-Branch Junction

Authors:
D Sellier, J Harrington

Research Provider:
Scion

This document is Confidential
to FFR Members

Date: September 2010

TABLE OF CONTENTS

EXECUTIVE SUMMARY	1
INTRODUCTION	2
METHOD	3
Overview	3
Parametric Studies.....	3
Primary Growth	3
Secondary Growth	4
Finite Element Analysis.....	4
Post-processing	7
RESULTS	9
Phenomenology.....	9
Effects of Stem Radius.....	9
Effects of Insertion Angle	11
Effects of Branch Radius.....	12
Effects of Foliage Weight	14
CONCLUSION.....	17
REFERENCES	17

Disclaimer

This report has been prepared by New Zealand Forest Research Institute Limited (Scion) for Future Forests Research Limited (FFR) subject to the terms and conditions of a Services Agreement dated 1 October 2008.

The opinions and information provided in this report have been provided in good faith and on the basis that every endeavour has been made to be accurate and not misleading and to exercise reasonable care, skill and judgement in providing such opinions and information.

Under the terms of the Services Agreement, Scion's liability to FFR in relation to the services provided to produce this report is limited to the value of those services. Neither Scion nor any of its employees, contractors, agents or other persons acting on its behalf or under its control accept any responsibility to any person or organisation in respect of any information or opinion provided in this report in excess of that amount.



EXECUTIVE SUMMARY

Past work on the modelling framework for mechanobiology of wood formation focused on modelling the physiological aspects of tree growth – namely carbohydrate production and transport and water transport. These parameters, combined with the 3D surface growth model, laid the foundations of the first-generation growth model. This year, milestones focus on modelling tree biomechanics. The eventual outcome of the IFS Objective 2 modelling framework being developed at Scion is develop a computer model of a whole tree by integrating knowledge on the mechanisms of wood formation.

The computer model developed to simulate the mechanical behaviour of branch insertions in the stem is part of the IFS Objective 2 modelling framework. It relies in large part on the tools previously developed to simulate tree growth and biomechanics. The model of stem-branch mechanics adds the capability to simulate the influence of branches on stem development and its internal structure.

Tree branches transfer their own weight and the weight of branches and foliage they support to the trunk. The load transfer locally perturbs the mechanical state of the stem surface around the point of branch insertion. Mechanical variables also affect the activity of the vascular cambium – the tissue that produces wood. Investigating the mechanical perturbation associated with branch presence is a crucial step towards understanding local perturbations in wood properties. This project consists of a series of parametric studies. In these studies, one parameter is varied at a time to examine its effect on wood properties. In this instance, we determined the effect of branches on the mechanical state of the stem surface where the vascular cambium is located.

Numerical experiments have been repeated by varying factors affecting the shape of an idealistic branch-stem junction. Those factors include angle of insertion, branch radius and foliage mass. Depending on those characteristics, the branch influence on stem mechanics can be weak or strong. However, such an influence always remains local.

The modelling framework developed in IFS Objective 2 now has the numeric tools to simulate the effect of branches on wood properties. That effect of branches on stem wood properties is highly localised to the branch insertion point on the stem. However, despite being local, perturbations induced by branches can be strong and have important effects on log value. The model parameterisation is still highly simplistic with regards to the complexity of wood patterns inside whorls. Further studies will be needed, such as incorporating the effect of the grain on complex wood patterns and mechanics of branch-stem junctions.

INTRODUCTION

Trees, like human-engineered structures, are subject to mechanical loads throughout their lifetime. In contrast with the latter, trees grow and adapt to forces during growth^[1]. Adaptations potentially affect both tree shape and wood properties^[2]. Among all possible adaptations, particularly interesting ones take place at the junction between tree trunk and a branch.

The physical insertion of a branch into the supporting axis is a local perturbation, both physically and mechanically. Wood fibres of the trunk are re-oriented in a way that looks as though the grain flows around the branch. This flow analogy has been used to create models of grain orientation^[3],^[4]. Shigo^[5] described a succession of branch and trunk fibres, alternately layered (see also Foley^[6]). However, wood patterns can be more complicated in nature: woods produced by the trunk and the branch may become indistinguishable and with a wide range of variation.

A special reaction wood forms within the junctions, which has been referred to axillary wood^[7],^[8]. Several types of axillary wood exist. In most cases the axillary wood shows a darker colour than normal wood and an increased cell wall thickening^[7]. The branch-stem junction is also complex mechanically. Firstly, vascular cambia of both supporting and supported organs compete to occupy space and exert contact forces onto each other. Secondly, weight, by being transferred from the branch to the stem, induces localised stresses at the interface. The interface can thus be seen as a zone of frailty where strain and stresses are concentrated. On the other hand, nodal swelling – by making the branch-stem transition less abrupt and less angular – and axillary wood both mitigate the mechanical perturbation associated to the branch insertion^[9].

In this study, some aspects of the branch-stem junction will be investigated, and previous work reported in FFR reports RO43, RO50, RO053 and RNT010 will be built on. Our primary aim is to infer the nature and the amplitude of the mechanical perturbation caused by a branch as a function of its characteristics (basal radius, carried weight, angle of insertion). Most complexities such as fibre re-orientation, material adaptations, and contact forces are not accounted for. Effects of varying whorl configurations are evaluated by computer simulations. Mechanical behaviour of a branch-trunk junction is modelled using the Finite Element method. The whorl itself is simulated using the numerical tools previously developed as part of the IFS Objective 2 '*mechanobiology of wood formation*' modelling framework.

METHOD

Overview

The aim of this study is to develop the tools to carry out numerical simulations which will later be used to investigate the real behaviour of whorls.

The sequence of methods to study the mechanics of a stem-branch junction are:

1. Provide a parameter set defining the whorl geometry.
2. Create a whorl skeleton (primary growth).
3. Simulate wood formation (secondary growth).
4. Perform a finite element analysis, given applied loads.
5. Extract stress/strain on tree stem surface.

If an iterative growth process is taken into account, the steps 1-5 are repeated for each growth cycle.

Parametric Studies

Whorls are defined by multiple parameters. Those are length of stem section, height of branch insertion, stem and branch radii, whorl age, branch length, and foliage mass. The framework for defining parameters is extensible. Each parameter set corresponds to a particular whorl configuration, and all parameter values are accessible throughout a simulation.

To carry out a parametric study, one must generate different parameter sets. In our approach, parameters are stored in file with a .par extension. The header line defines the parameter names and each subsequent line forms a parameter set by giving parameter values corresponding to the treatment to test. The parstudy.py script is then invoked with the .par file as argument in order to run the parametric study. Remaining actions are automated. Usage of the parstudy.py script is self-documented.

Usage: parstudy.py [options] treatments.par

Options:

- | | |
|-------------------|--|
| -h, --help | show this help message and exit |
| -f, --force | force creation and FEA of each parameter configuration |
| -i, --incremental | apply loads incrementally |
| -b, --branchonly | apply loads on branch only |

For each treatment, i.e., parameter set, a file with the .ana extension (which stands for analysis) is produced. The file contains a statistical summary of key mechanical variables on the tree stem surface. Colour strain and stress maps are also being produced.

Primary Growth

The elongation and branching of shoots is simulated by the wire component of the IFS2 modelling framework. This component has been specially developed as part of this milestone to generate archetypal tree structures from user-defined elongation and branching models. The wire component's name stands for wireframe in that only the longitudinal dimension of shoots is modelled in an explicit manner. wire generates tree architectures that are encoded as directed graph and stored in a file format which is a simplified version of Multiscale Tree Graph file format [10]. The wire component makes minimal assumptions regarding the functioning of the apical meristem and the complexity of architectures it can produce is directly linked to the underlying

theoretical branching and elongation models. During this exercise, models attached to wire were fairly simple in that they only needed to yield a short stem section with a single inserted branch.

Secondary Growth

Radial enlargement of tree shoots is simulated using the pre-existing growth component of the *IFS objective 2* modelling framework. Radial growth speed is distinct for both branch and trunk surface compartments. Speed values remain constant for the growth period. Figure 1 shows the whorl at the final stage of growth. Wood formed is **homogeneous** but with physical properties that do not vary with direction (**isotropic**), as the modelling framework does not yet include property models. This is a very strong hypothesis, and the reader must exert caution in interpreting the result.



Figure 1: A whorl composed of a stem section and a single branch simulated using the IFS o2 modelling framework.

Finite Element Analysis

Domain triangulation

A mesh of 3D solid elements is generated from the implicit whorl representation produced after the secondary growth step. Mesh generation is done using both the *mech* module and the *mesh* library of the IFS modelling framework. Both components already existed but have been extended during the course of this study. Those components use the VTK (<http://www.vtk.org>) Delaunay triangulation routine. The Delaunay triangulation is a computational geometry structure that subdivides the domain in triangles or tetrahedra. The triangulated domain is generated from a set of points that belong to the domain. In 3D, the Delaunay triangulation does not yield a unique subdivision. Moreover, the VTK routine is not constrained. Although it provides some degree of control on the shape of the tetrahedra being generated, it is not possible to strictly enforce the boundaries of the domain. Because of this, some tetrahedra are not physically relevant: they lie outside the domain boundaries. Those extra elements can be seen in Figure 2. They are located at the very junction of the stem and the branch and must be removed after the tetrahedral meshing is done. A filtering routine has been added to the *mesh* library to mitigate the issue. Domain triangulation also causes decimation of few points located on the surface of the shoots. It is a minor annoyance which hasn't been corrected. Fixing the issues related to triangulation would

require employing and possibly developing other Delaunay routines, a not-so-trivial task which has to be subordinated to the treatment of the matter at hand.

Another issue was the presence of additional irregularities at the branch-stem interface that are independent of the meshing tools. Those irregularities are contained within element size (see Figure 3). They are inherent to the way multi-compartment surface growth is modelled and there is no obvious alternative modelling approach. The simplest way to handle the issue is to increase grid resolution and thus decrease the size of the irregularities. To counterbalance the increased number of mesh elements, a *hybrid* mesh option has been added to the mesh component. Hybrid refers to the fact that the inner volume of shoot organs is meshed with hexahedra instead of tetrahedra. The hybrid approach allowed decreasing the overall number of elements by a factor of four. A final addition to the mesh library is the capability to generate quadratic elements for either hybrid or fully tetrahedral approaches.

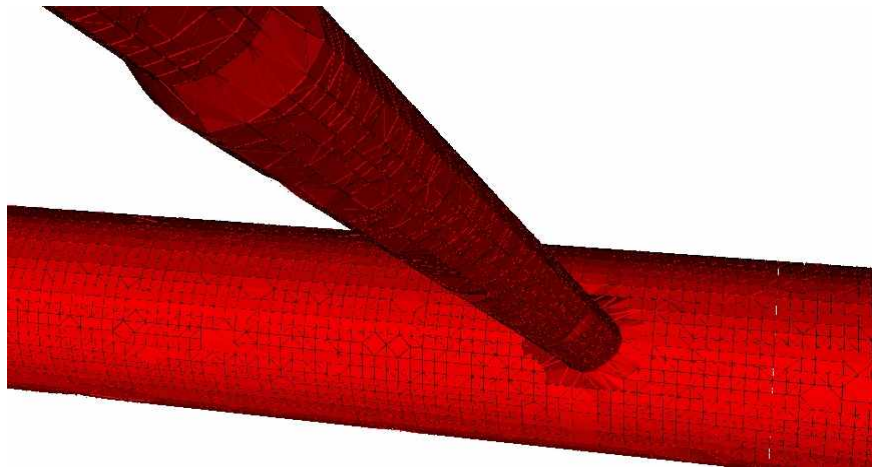


Figure 2: Undesired elements at the very branch-stem junction appear as a result of a shortcoming in the meshing process. Those elements connect points on the stem surface and the branch surface but elements themselves are outside the surface. They are filtered out afterwards.

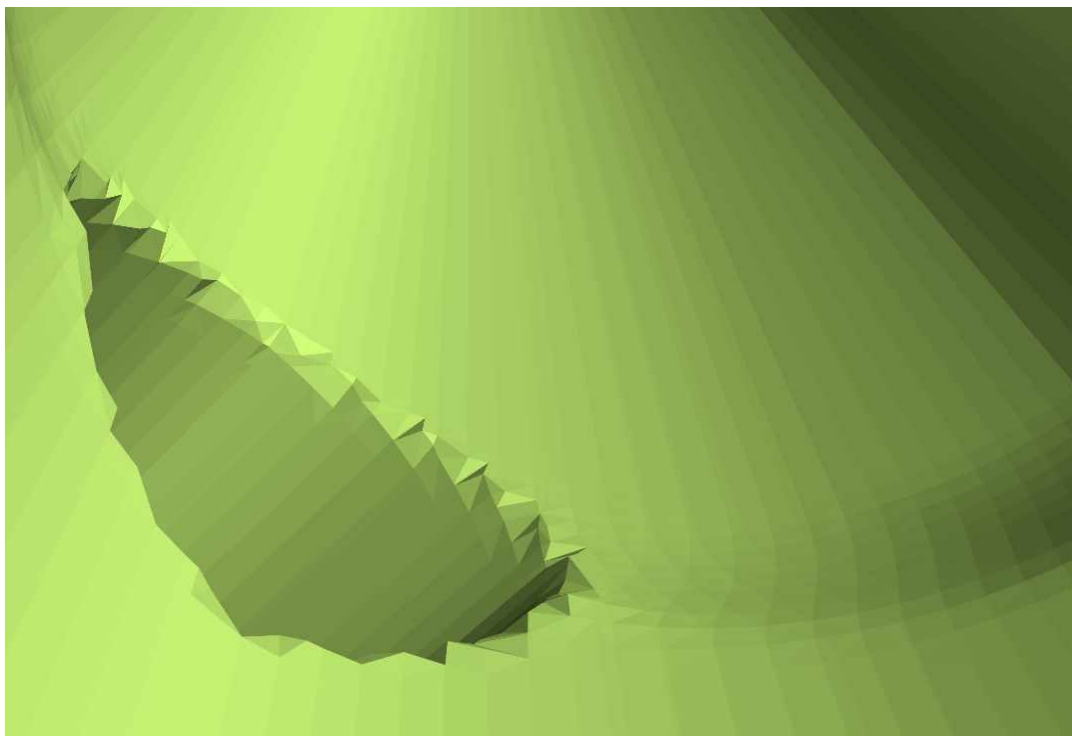


Figure 3: Cambial layer seen from inside showing the second kind of irregularities observed at the stem-branch interface. Mesh size is 5 mm.

Convergence

A convergence study was performed to determine the optimal mesh in terms of accuracy and computational time. Figure 4 shows computed longitudinal strain, ϵ_L , on stem surface as element size varies. Gravitational load is applied to the branch only. The median value, 5% and 95% percentiles of ϵ_L were studied. The median remains stable for all tested element sizes. The 5% percentile of longitudinal deformation oscillates around a value equal to $275 \mu\text{def}$, (Micro deformations are 'units' for deformation). Oscillations are not necessarily errors induced by the FEM. Like any numerical method, the Finite Element Method yields an approximation of the theoretical solution. Refining mesh resolution or using better elements (like quadratic over linear) contribute to reduce the error between the approximated solution and the theoretical one. The method is said to converge when further mesh refining does not increase accuracy any more. The similar values obtained with linear and quadratic elements tend to show the FEM already converged. It is more likely that element size affects accuracy of the level set method for branch growth. Error assessment is further complicated by the fact that tested quantities are statistical and depend on spatial sampling of the observation window, which obviously varies with element size.

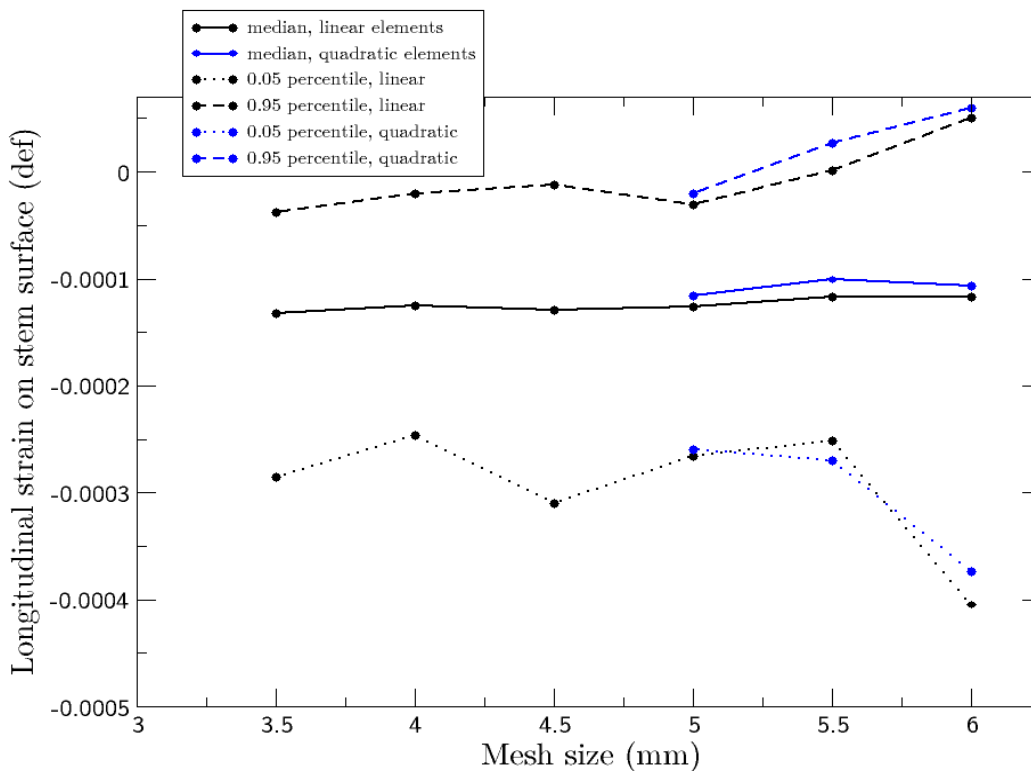


Figure 4: Surface longitudinal strain expressed as a function of element size. Results with quadratic elements are available only for lower resolutions (i.e., higher element size).

Figure 5 shows computational times associated with each simulation performed during the convergence study.

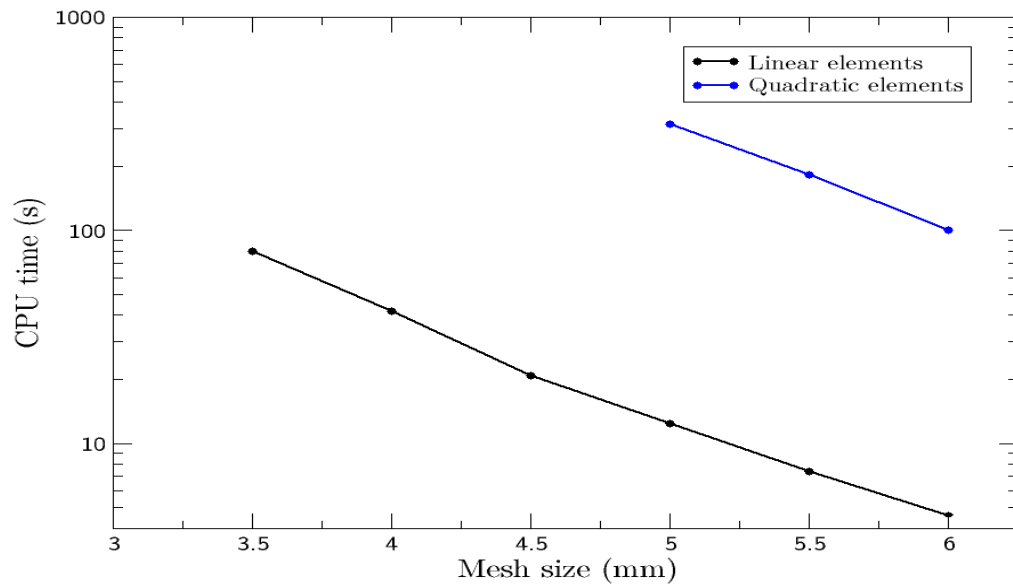


Figure 5: Computational time on a personal computer as a function of mesh characteristic size. Computations with quadratic elements for an element size less than 5 mm ran out of available memory and could not be completed.

Conclusions:

- there is little difference observed between linear and quadratic elements,
- there is no obvious benefit in decreasing element size in terms of accuracy,
- there is an obvious drawback in decreasing element size in terms of computational time,
- use of quadratic elements yields much higher computational times

All subsequent FE computations were carried out using linear elements, with an element size of 5 mm.

Calculix (Guido Dhondt and Klaus Wittig, *Calculix*) is used to carry out FE analyses. FE models can also be read and analysed using ABAQUS (*ABAQUS*, Providence RI, USA: Simulia).

Post-processing

Strain and stress tensors are computed for each simulation. In this study we primarily analysed the longitudinal strain, which is a mechanical variable sensed by the vascular cambium^[11] and the Van Mises stress criterion which provides an overall estimation of the stress level by combining all components of the stress tensor and which can be used to evaluate the risk of fracture. While the result of analysis is three-dimensional (Figure 6), only deformations and stresses on the surface of the tree stem are relevant, since we are interested only in determining the mechanical environment of the cambium.

Numeric tools have been developed to extract Calculix results, unroll the tree stem surface and analyse and/or plot strain or stress maps for a given observation window (see Figure 7 for an example). All those tools are written in Python programming language and kept in a versioned repository that is separate from the main modelling framework. They are designed to be re-used. That is, if grain orientation becomes available in the future as attribute data, repeating parametric studies of the branch-stem junction will require no modifications at the level of the post-processing chain.

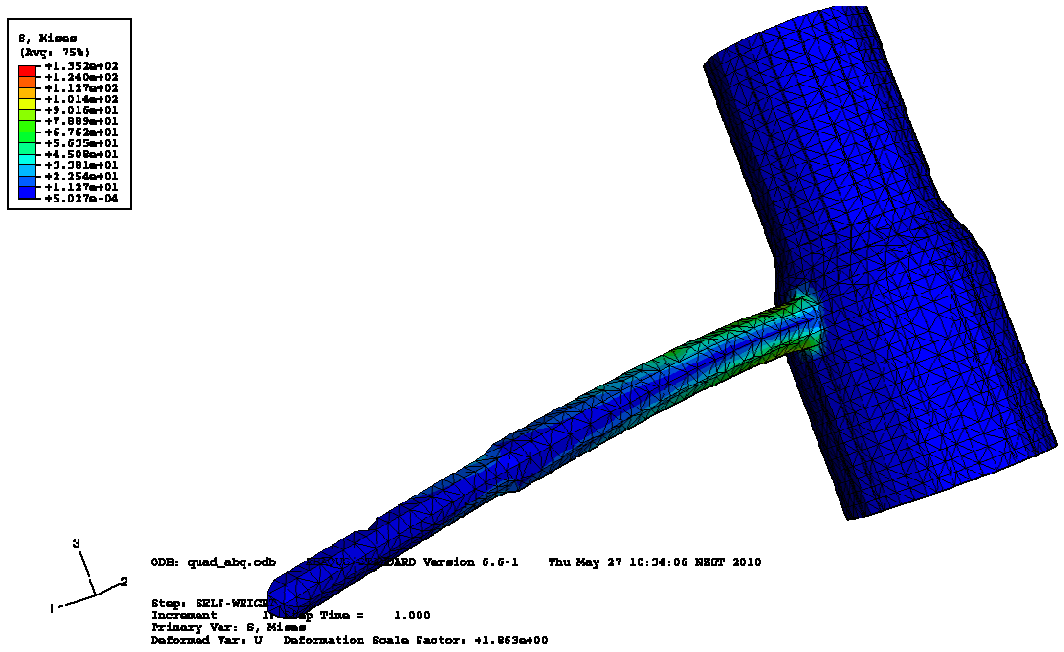


Figure 6: 3D view of the simple whorl configuration used in this study.

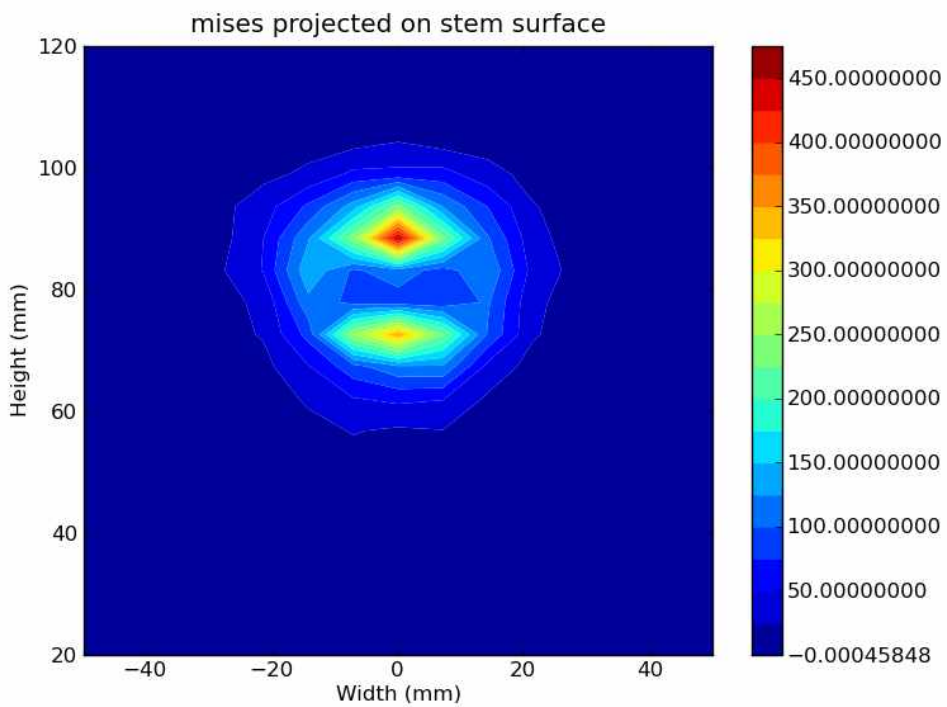


Figure 7: Convolved view of the Mises stress criterion (kPa). The load case differs from the previous figure.

RESULTS

Phenomenology

This section describes how a branch alters the mechanical state of the tree stem surface. As a branch bends under its own weight and the weight of the foliage and higher order axes it supports, its lower side is compressed while the upper side is under tension. As shown by maps of longitudinal strain and stress in Figure 8, bending is transferred to the stem. Surface fibres are under tensile deformation/stress above the point of insertion and under compression just below.

One should note that asymmetric loading is also possible, although only the case of straight branches and symmetric loading have been investigated in this study. Asymmetric loading will induce torsion and cause additional shear stress on the stem surface.

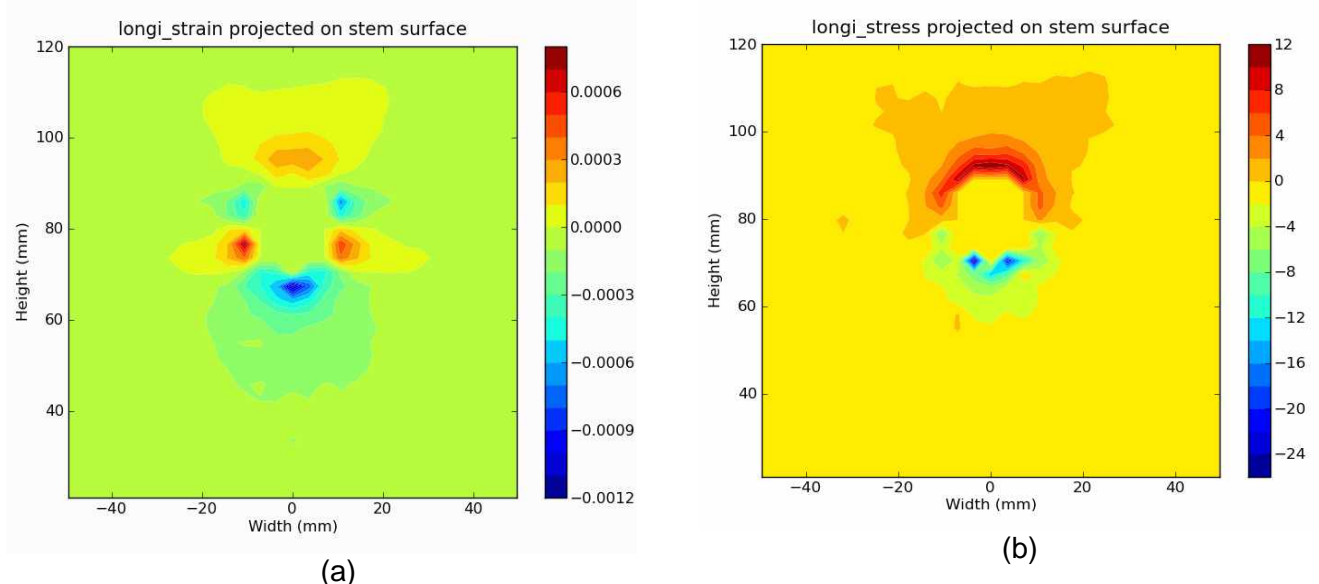


Figure 8: 2D maps of longitudinal (a) deformations (-) and (b) stresses (kPa) on the surface of tree stem. Branch radius is 10 mm.

Figure 8 also highlights that the area on the stem surface that is mechanically perturbed by the branch insert is range-restricted to several branch diameters. We will see however that the perturbed area varies in size depending on branch characteristics.

Effects of Stem Radius

The effect of the stem radius on surface stress is investigated. Mechanical simulations are done without considering the growth incremental process. Instead, the weight of the branch is applied at the end of the growth period over the entire branch volume. For all simulations, the branch radius remains equal to 10 mm.

Two criteria are considered to characterise mechanical stresses on the stem surface:

1. Percentiles at 5%, 50% and 95% of the von Mises stress criterion. One could have used minimum, mean, and maximum values, respectively. However the latter are less robust, especially in the light of the minor mesh irregularities caused by the Delaunay triangulation and local singularities at the stem-branch junction.
2. Area under the isocontours for Mises stress values equal to 12, 16 and 20 kPa. Those three values are chosen high enough so that the isocontour fits in the observed region but low

enough so that isocontour are continuous. Isoarea computation is an attempt at evaluating the geometrical extent of the mechanical perturbation caused by the branch. The stem surface is observed on a window at +/- 50 mm on both sides of the branch insertion point, and at +30/-70 mm along the vertical direction unless specified otherwise.

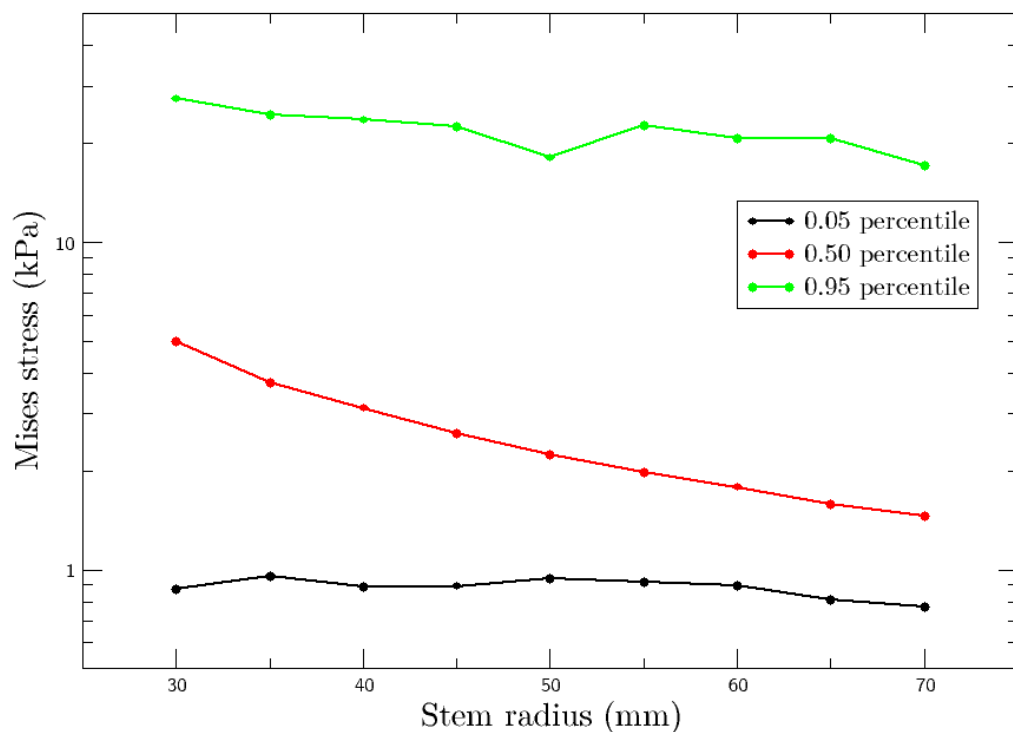


Figure 9: Evolution of surface Mises stress as a function of stem radius. Mechanical loading considered is branch self-weight only, which is constant for all simulations.

Figure 9 shows that both the 5% and 95% percentiles of the Mises stresses are not influenced by the stem radius value. On the other hand, the median stress level drops markedly with stem radius. This is expected since the branch weight is distributed over a cross-section that increases with stem radius. The effect is quite pronounced since the median stress is reduced by a factor of five over the tested range of stem radii.

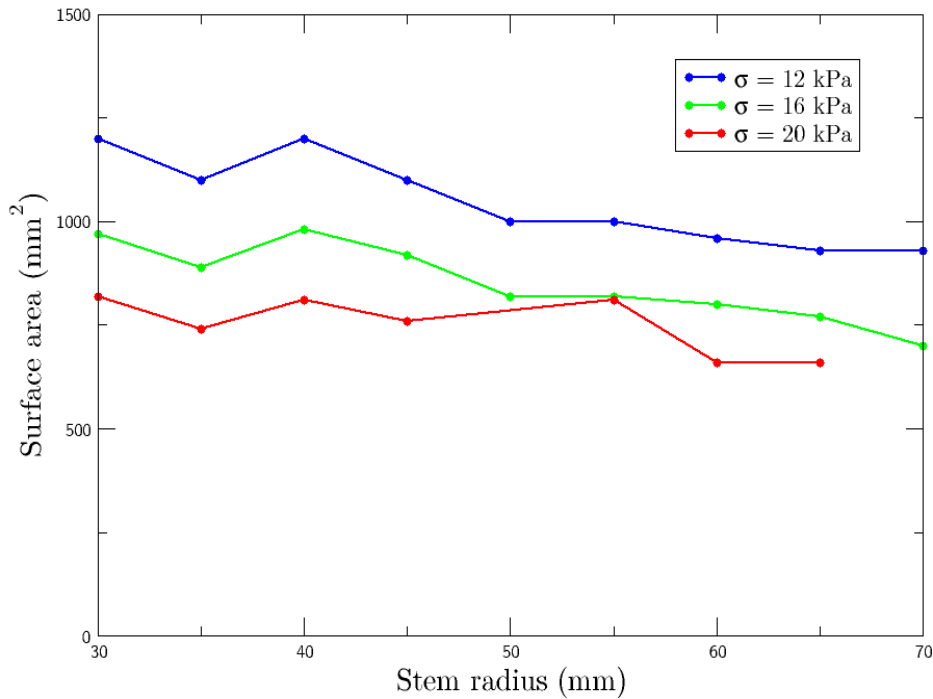


Figure 10: Evolution of the area of the high stress zone induced by the branch as a function of stem radius.

Figure 10 depicts a more interesting behaviour. Areas around the branch with a Mises stress higher than 12, 16 and 20 kPa, respectively, all decrease with an increasing stem radius. However, the decrease is relatively much smaller than the overall decrease of the median stress on stem surface. Therefore, surface stresses in the immediate surroundings of the branch insertion are only weakly affected by stem size. In other terms, a branch of a given size has an absolute influence on the stress field that does not vary. However that influence will be relatively important for a stem of small size and relatively non-important for a larger one.

Effects of Insertion Angle

Figure 11 shows a drastic increase in surface stress as the insertion angle of the branch relative to the stem increases. As the branch gets closer to the vertical direction (i.e., smaller angle), the effects of gravity are minimised. On the other hand, lever arm is maximal for horizontal branches and so is the load transferred to the stem. Because of the lever arm effect, branch length will interact with insertion angle to alter the amplitude of surface stress. There also exists a secondary effect. With a decreasing insertion angle, the branch intersection with stem surface becomes more and more elliptical. The associated increase of area must contribute to reducing the local magnitude of stresses since the load is transferred over slightly larger section. This effect is expected to be small in front of changes in bending moment associated to branch orientation.

The stress increase is particularly pronounced for the 5% and 95% percentiles: approximately an order of magnitude higher. The increase of the median stress is less marked. Those aspects depict a skewing of the stress distribution as the insertion angle increases. The highest levels of stresses are less wide-spread as the branch is closer to the horizontal; transition from high to low stress levels is steeper.

Effects of Branch Radius

To study the effects of branch radius on the surface stress field, incremental growth was considered. Branches were grown over a period of 5 years to reach the target branch radius, ranging from 10 to 20 mm. Growth rates were assumed to be constant over the period. Branch radius and branch mass increase with age, whereas branch length does not change. Because the growth rate is constant, the increment in mass and volume is pseudo-linear. The stem is also growing, not only the branch.

The gravitational load increases proportionally with mass (no foliage is considered at this point, only wood). Surface strains induced by cell maturation are taken into account. Maturation strains are also proportional to the volume of newly formed wood and therefore increase linearly with time, like self-weight. Increased loads translate to an increase in both 5% and 95% percentiles of Mises stress over time (Figure 12). Interestingly, the median stress (Figure 13) does not change, an effect which may be attributed to the fact that branch size gets larger relatively to the observation window. It may also reflect a change in the statistical distribution of the surface stress.

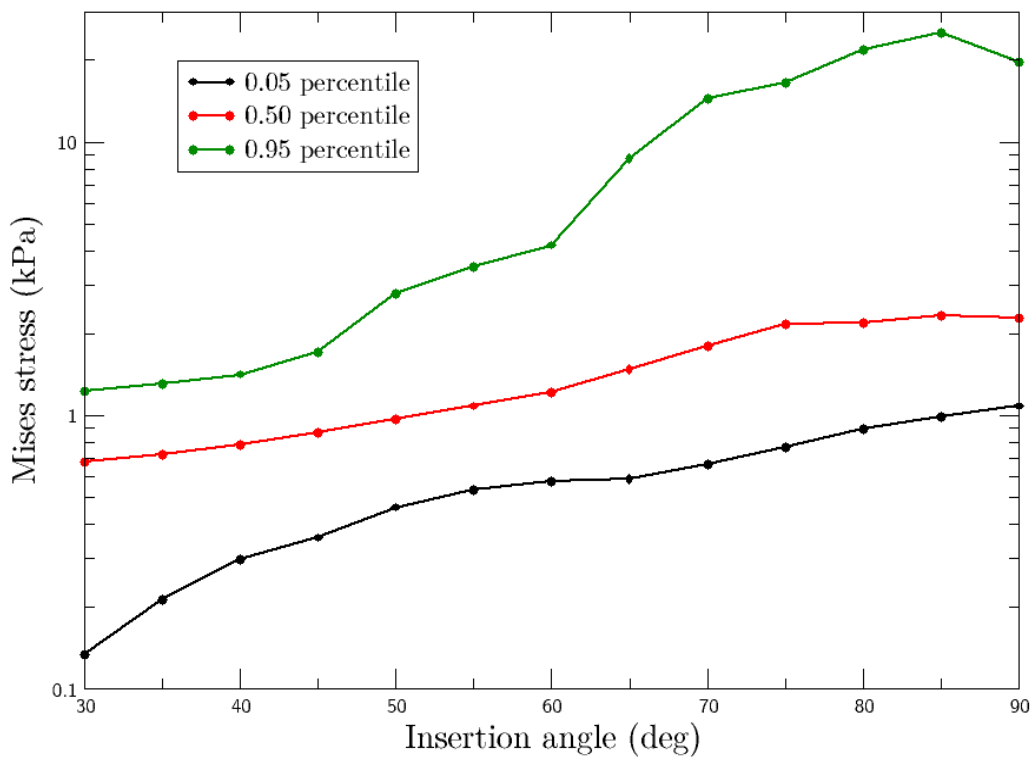


Figure 11: Evolution of surface stress (Mises, kPa) as a function of branch insertion angle.

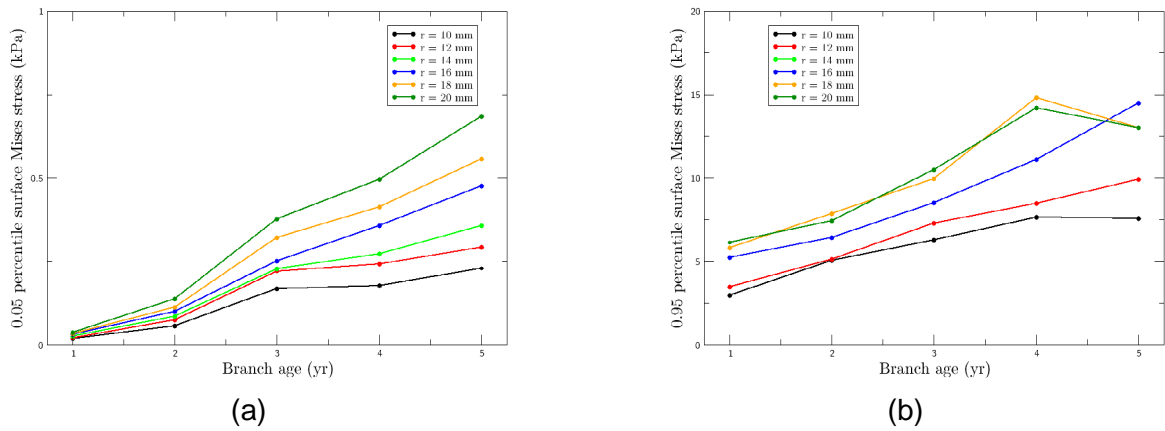


Figure 12: Evolution of (a) 5% and (b) 95% percentiles of the surface stress (Mises, kPa) as function of time for different branch radii (radius value is at the age of 5 years).

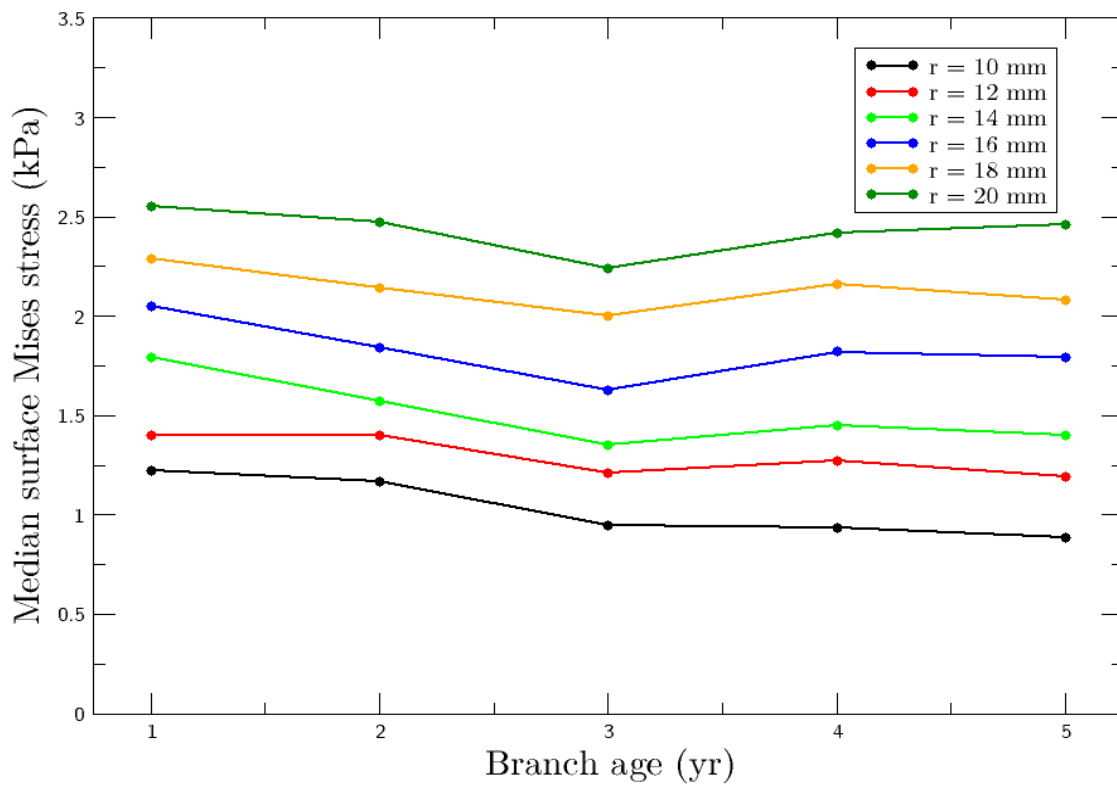


Figure 13: Median stress on stem surface induced by branches of different final radius over a period of five years.

Looking at the area occupied where stress is higher than 12 kPa (Figure 14), several points emerge:

1. The high stress zone increases in size with age for any branch radius.
2. The larger the branch radius, the larger the high stress zone is.
3. Except for the first year, the area of the high stress zone around the branch is proportional to the increase in branch basal area (not shown).
4. The high stress zone is relatively larger for a small branch than for a large one (but not absolutely).

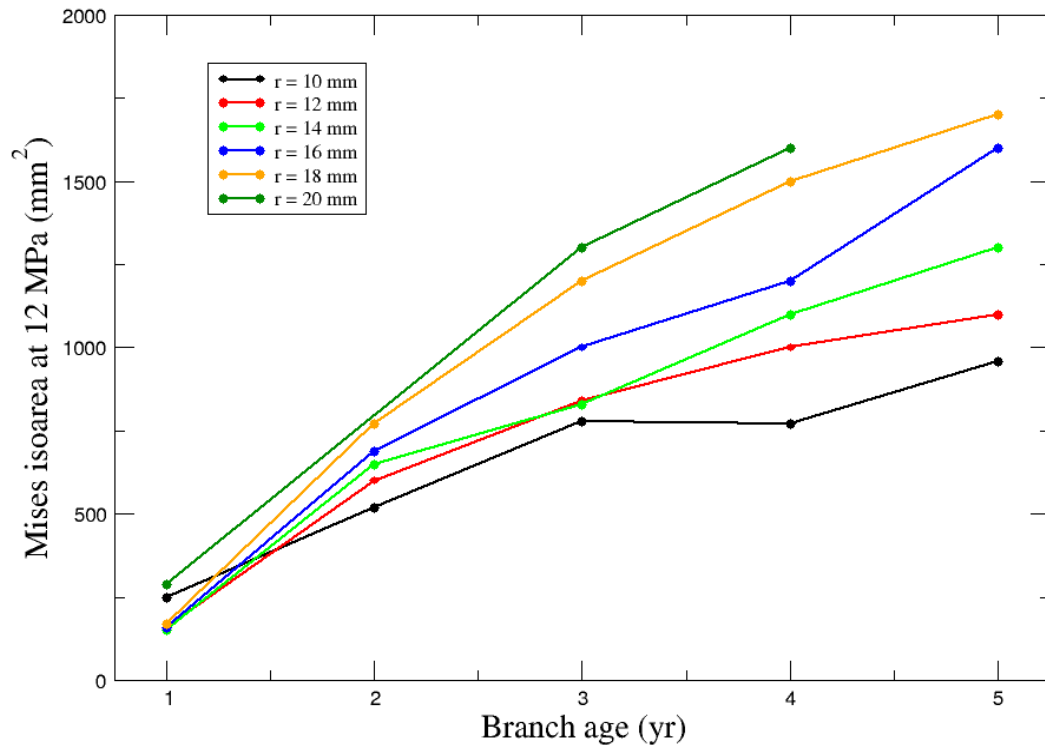


Figure 134: Area occupied by the 12 kPa- stress isocontour as a function of branch age.

All those points make it clear that mechanical stresses induced by the branch primarily depend on branch size, in that branch size determines the amplitude of the mechanical loads (weight and maturation). Let us consider branch size and mechanical loading varying independently.

Effects of Foliage Weight

In this parametric study, foliage mass varies from 100 to 500 g. It is modelled by a point load at $\frac{2}{3}$ of branch length. Incremental growth is not taken into account for the sake of simplicity (branch lengthening would have side effects). As branch length is considered a constant, and no loads other than foliage weight are taken into account, variations of foliage weight induce proportional changes in bending moment.

Median and lower stress percentile are unaffected by branch radius (Figure 15). However, higher stress values are reached with a smaller branch radius. The larger the branch basal area, the more diffuse is the stress field at the vicinity of the insertion. In nature, one may argue that the biggest branches are also the heaviest. Notwithstanding, it is interesting to note that the increase in geometrical dimensions partially compensates for the increase in weight by reducing stress concentration.

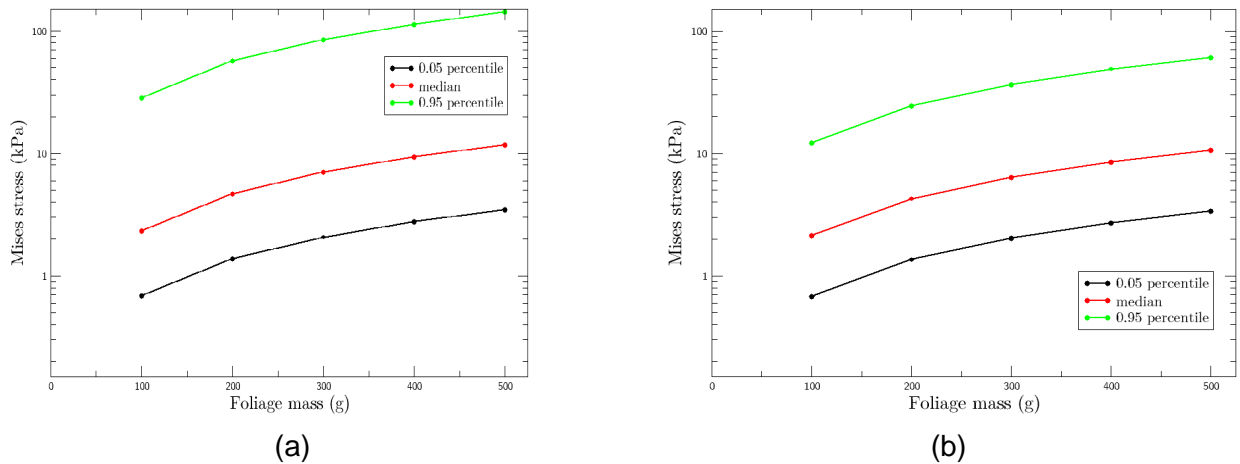


Figure 145: Surface stress percentiles (5%, 50%, and 95%) for a foliage mass varying from 100 to 500 g and branch radius equal to (a) 10 mm and (b) to 20 mm.

Twelve to twenty kPa isocontours enclose the base of the branch in for a branch radius of 10 mm (Figure 16a). For low load levels (0.1 kg, 0.2 kg) and a larger branch radius this is not the case (Figure 16b). High stresses form pockets just above and below the insertion. For high load levels, those two pockets merge into one which surrounds the branch base.

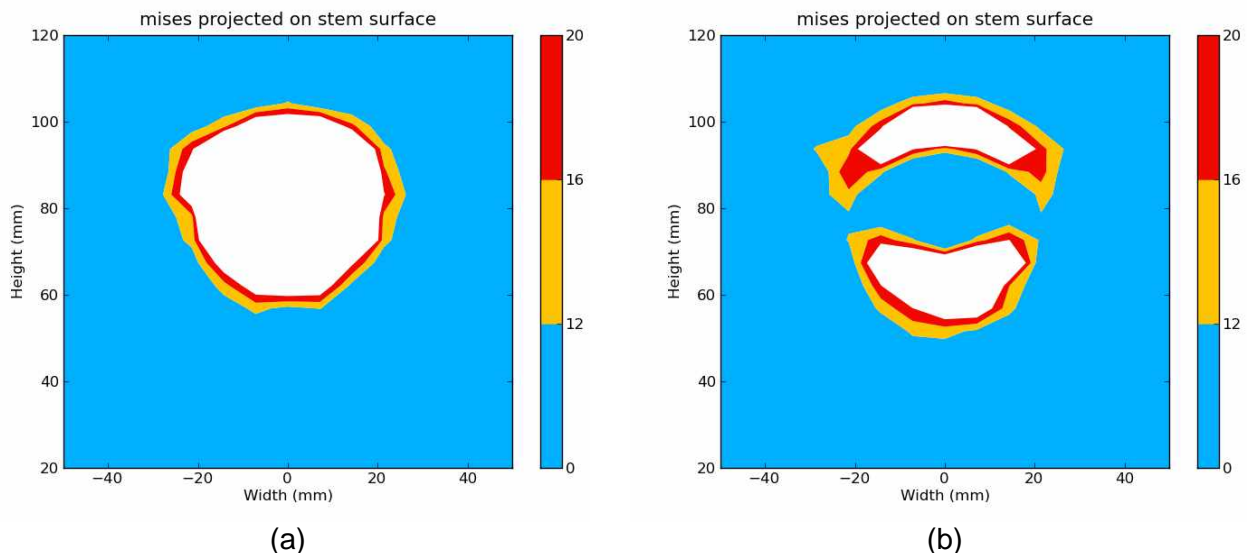
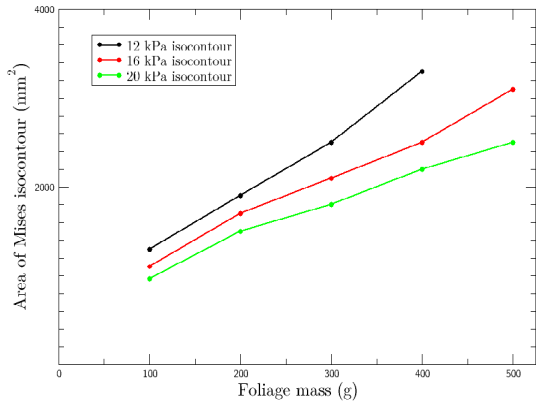
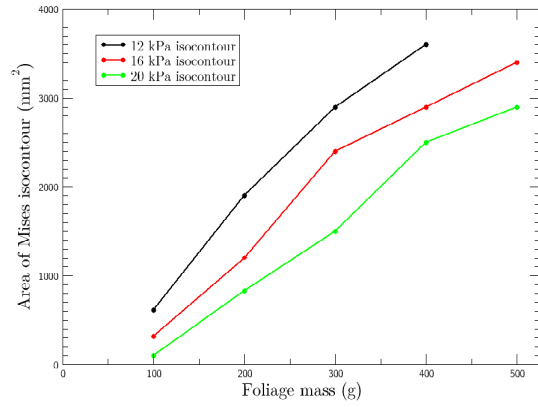


Figure 156: Distribution of Mises stress on stem surface around the branch insertion. In the case of (a) the branch with a small radius ($r = 10$ mm), stress isocontours enclose the branch base; (b) For the larger branch ($r = 20$ mm), the isocontours are not continuous and form two pockets, one above and one below the branch.

Stress isocontours evolve differently for both branch radii according the amount of supported foliage (Figure 17). At low load levels, the area covered by any stress isocontour is relatively smaller for the large branch than for the small one. This is because the area of the zones where stresses are higher than 12 kPa does not surround the base of the branch. When foliage mass increase As mass foliage increases, 12-20 kPa becomes of a magnitude similar to that of the median stress. Isocontour areas are then equivalent to the ones measured for the small branch, possibly higher.



(a)



(b)

Figure 167: Evolution of isoareas as a function of supported foliage mass for both two branches with a radius equal to (a) $r = 10$ mm and (b) $r = 20$ mm.

CONCLUSION

A model has been developed and applied to study the mechanics of the branch-stem junction. Emphasis was to determine surface stresses and deformations as those variables affect the activity of the vascular cambium and therefore wood formation. Results have shown a very high stress magnitude on the stem surface at the immediate vicinity of the branch insertion, in particular directly above and below the branch. Stress then decreases very rapidly away from the insertion point. Such a decrease is even more pronounced if the branch is small relative to the stem. Stress and deformation magnitude around a branch appeared to depend directly on the weight or maturation forces applied to the branch. However, an increased basal area was shown to reduce the local stress concentration without changing the overall mechanical load transferred to the stem.

However, wood material as simulated in this study is extremely simplified and by no means matches the material formed in real trees. The study was conceived as a test ground to develop tools necessary to understand the branch-stem junction. Results show this can be done but should *not* be used to support any decision or produce knowledge until more realistic material descriptions become available in IFS Objective 2 modelling framework.

The branch-stem junction model is an important step to look at tentative cambial responses to strain/stress state and investigate connections with growth rate and cell characteristics. Those aspects will be the subject of future studies.

REFERENCES

1. Mattheck, C., *Design in Nature: Learning from Trees*. 1998: Springer.
2. Telewski, F.W., *Wind and trees*, in *Wind and trees*. 1995, Cambridge University Press. p. 237–263.
3. Phillips, G.E., J. Bodig, and J.R. Goodman, *Flow-grain analogy*. *Wood Science*, 1981. **14**(2): p. 55-64.
4. Kramer, E., *Wood Grain Pattern Formation: A Brief Review*. *Journal of Plant Growth Regulation*, 2006. **25**(4): p. 290-301.
5. Shigo, A.L., *A New Tree Biology: Facts, Photos, and Philosophies on Trees and Their Problems and Proper Care*. 2nd ed. 1989: Shigo & Trees, Associates.
6. Foley, C., *Modeling the effects of knots in Structural Timber*. 2003: Structural Engineering.
7. Pfisterer, J.A. and H. Spatz, . 2006, STFI-Packforsk AB: Stockholm. p. 61-66.
8. Hartig, J.A. et al., . 2006, STFI-Packforsk AB: Stockholm. p. 67-72.
9. Müller, U., W. Gindl, and G. Jeronimidis, *Biomechanics of a branch – stem junction in softwood*. *Trees - Structure and Function*, 2006. **20**(5): p. 643-648.
10. Godin, C. and Y. Caraglio, *A Multiscale Model of Plant Topological Structures*. *Journal of Theoretical Biology*, 1998. **191**(1): p. 1-46.
11. Coutand, C. and B. Moulia, *Biomechanical study of the effect of a controlled bending on tomato stem elongation: local strain sensing and spatial integration of the signal*. *J. Exp. Bot.*, 2000. **51**(352): p. 1825-1842.